ELSEVIER

Journal of Power Sources 54 (1995) 470–474

JOURNAL OF POWER SOURCES

Reversible lithium intercalation in alkali metal vanadium bronzes ($M_xV_6O_{13+\delta}$, where M = K, Rb or Cs)

E. Andrukaitis

Directorate Research and Development Air, Research and Development Branch, 101 Colonel By Drive, Ottawa, Ont., K1A OK2, Canada

Abstract

Thermal treatment of electrochemically prepared crystalline solid solutions of ammonium hexavanadates containing K, Rb or Cs formed adherent electrodes on a conducting substrate without the need for binders. These $M_xV_6O_{13+\delta}$ bronzes where M = K, Rb or Cs belong to the ternary system V_2O_4–V_2O_5–M_2O. By controlling the electrodeposition/decomposition processes, various alkali metal to vanadium ratios (0.0 to 0.65) and oxygen to vanadium ratios (2.2 to 2.5) were studied. The $RbV_6O_{13+\delta}$ bronzes have not been studied, they are reversible to lithium insertion. For maximum capacity, only small amounts of the alkali metal could be present. Voltage plateaus for small M/V ratio bronzes were similar to V_2O_5 for electrodes made by thermal decomposition in air, and to V_6O_{13} when heated under a vacuum atmosphere.

Keywords: Lithium intercalation; Vanadium; Alkali metals

1. Introduction

Vanadium oxides that have made the largest advances in practical applications for rechargeable lithium battery systems, are V_2O_5, LiV_3O_8 and V_6O_{13} [1]. Intercalation using hetero-atom materials, in which another metal is added to the vanadium oxide may have some advantages over a pure vanadium oxide, since the solubility of vanadium oxides in non-aqueous electrolytes, such as propylene carbonate, is a problem. Vanadium pentoxide bronze phases of the form $M_xV_2O_5$, where M = Li, Na, K, Cs, Mg, Ca or Ag, were examined as insertion electrodes [2–7] and reversible intercalation depended on the guest cation species [3].

The thermal decomposition of the electrodeposited $(NH_4)_xM_{4-x}V_6O_{16}$, (M = K, Rb or Cs), $0 \leqslant x \leqslant 4$, to form $M_xV_6O_{13+\delta}$ bronzes for lithium insertion cathodes was examined. The deposition method forms an adherent crystalline bronze on a conducting substrate, without the need for inert binders [8,9]. The bronzes behave as reversible Li^+ intercalation cathode materials.

2. Experimental

Materials were cleaned and prepared as described previously [10]. Solutions for electrodeposition were prepared by adding MVO_3 (M = K, Rb or Cs) to a NH_4VO_3 solution at 50 °C [6]. Electrodeposits were formed on conducting substrates of a 150 grid nickel or stainless-steel mesh by cyclic voltammetry from +0.2 to −0.7 V with a saturated calomel electrode (SCE) at 50 mV/s for several hours. The deposits were decomposed at temperatures from 300 to 400 °C under air or vacuum atmospheres (1 mmHg). Electrodeposits were analyzed by inductively coupled plasma spectroscopy (ICP), chemical analysis and X-ray powder diffraction (XRD).

Electrodes were discharged and charged galvanostatically at a current density of 0.1 to 10 mA/cm^2 or by cyclic voltammetry from 0.1 to 1 mV/s (PAR Model 273 potentiostat). The cell consisted of a counter, working and reference electrodes of lithium metal, vanadium oxide bronze and lithium ribbon, respectively. The electrolyte was 0.5 M $LiClO_4$ in propylene carbonate (PC). The amount of lithium intercalated into the bronze was determined by chemical analysis and compared with the total charge passed.

3. Results and discussion

3.1. Nature of the thermally decomposed bronzes

Formation of electrodeposits with the general stoichiometry $M_xM'_{4-x}V_6O_{16}$, with M, M' = K, Rb, Cs or

SSDI 0378-7753(94)02127-O

NH_4, $0.0 \leqslant x \leqslant 4.0$, have been discussed previously [8,10]. Bronze phases of given M/V ratio were deposited on a metal mesh by cyclic voltammetry to form adherent vanadate deposits on a nickel or stainless-steel mesh. By controlling the amount of alkali metal present during the electrodeposition process and the V(IV)/V(V) ratio by heating under air or vacuum atmosphere, various $M_xV_6O_{13+\delta}$ electrodes, with $0<x<4.0$ and $0<\delta<4.0$, were formed. The $Rb_xV_6O_{13+\delta}$ bronzes were examined as cathode materials. Because of the similar ionic radius of the Rb^+ and NH_4^+ ions (0.149 and 0.146 nm) [8] electrodeposited bronzes were expected to form uniformly and adhere well to the conducting metal substrate. The trend in the XRD patterns for the $Rb_xV_6O_{13+\delta}$ and $Cs_xV_6O_{13+\delta}$ bronzes were similar to those for the $K_xV_6O_{13+\delta}$ bronzes [6]. Several major peaks (primarily in the *c*-axis direction) in the XRD patterns of the alkali metal bronzes shifted proportionally with the amount and/or the ionic size of the alkali metal present between the vanadium oxide layers [8]. A progression was observed in the bronze structure from parent oxides of either V_2O_5 or V_6O_{13} (depending on heat treatment) to the tetrametal hexavanadate bronze ($M_4V_6O_{16}$) [6,8].

The location of thermally decomposed bronzes in the ternary system V_2O_5–V_2O_4–M_2O, where M = K, Rb or Cs, were plotted in Fig. 1. In the diagram, the $M_xV_6O_{13+\delta}$ bronzes were expected to be found in an area with V_2O_5, d(V_6O_{13}), i($M_4V_6O_{15}$) and j($M_4V_6O_{17}$) as its vertices. From analysis, the bronzes lie in two V(IV)/(total M–V(IV)–V(V)) bands of about 5 to 15% for air-decomposed and 50 to 65% for vacuum-decomposed bronzes. Location of the bronze in the phase diagram appeared to be independent of the ionic size of the alkali metal.

The simultaneous differential thermal analysis (DTA), DTG and thermal gravimetric analysis (TGA) trace of an electrodeposited bronze with the stoichiometry $(NH_4)_{0.9}K_{3.1}V_6O_{16}$ is shown in Fig. 2(a). By heating the sample in air, the DTA trace has an endothermic peak at 287 °C and an exothermic peak at 377 °C. The observed mass loss of 1.6 mg on 55.27 mg sample (2.89%) agreed with the corresponding reaction:

$$(NH_4)_{0.9}K_{3.1}V_6O_{16} + 0.11O_2 \longrightarrow K_{3.1}V_6O_{15.76} + 0.9NH_3 + 0.45H_2O \quad (1)$$

for which the net loss is 2.87%. The DTA trace was similar to that for $(NH_4)_4V_6O_{16}$ [10], but the mass loss (removal of all the NH_3 and H_2O) continued to higher temperatures (about 475 °C at 10 K/min scan rate). The endothermic DTA peak corresponded to the loss of ammonia and water in region I and continued into

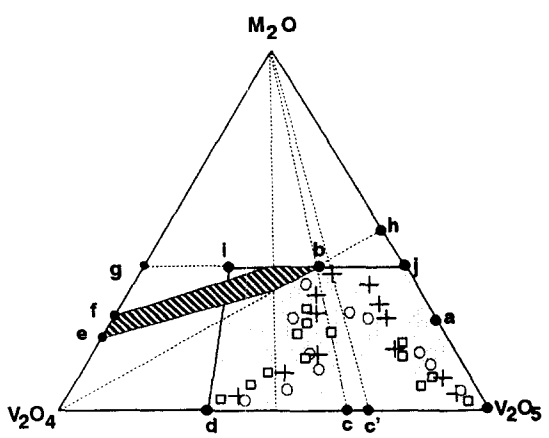

Fig. 1. Compositions of homogeneous phases in the system V_2O_5–V_2O_4–M_2O, where M = K, Rb or Cs: (a) $M_2V_6O_{16}$; (b) $M_4V_6O_{16}$ [11]; (c, c') V_3O_7, $V_3O_{7.07}$; (d) V_6O_{13}; (e, f, g) $M_2V_8O_{17}$, $M_2V_6O_{13}$, $M_2V_3O_7$ for M = K, Ref. [12]; (h) MVO_3; (i) $K_4V_6O_{15}$, and (j) $K_4V_6O_{17}$. Vertical hatching: results of Ref. [12] for M = K. Phases studied for lithium intercalation in this paper formed by thermal decomposition of $(NH_4)_xM_{4-x}V_6O_{16}$ at 350 °C in air or under vacuum: (□) $Cs_xV_6O_{13+y}$; (○) $Rb_xV_6O_{13+y}$, and (+) $K_xV_6O_{13+y}$.

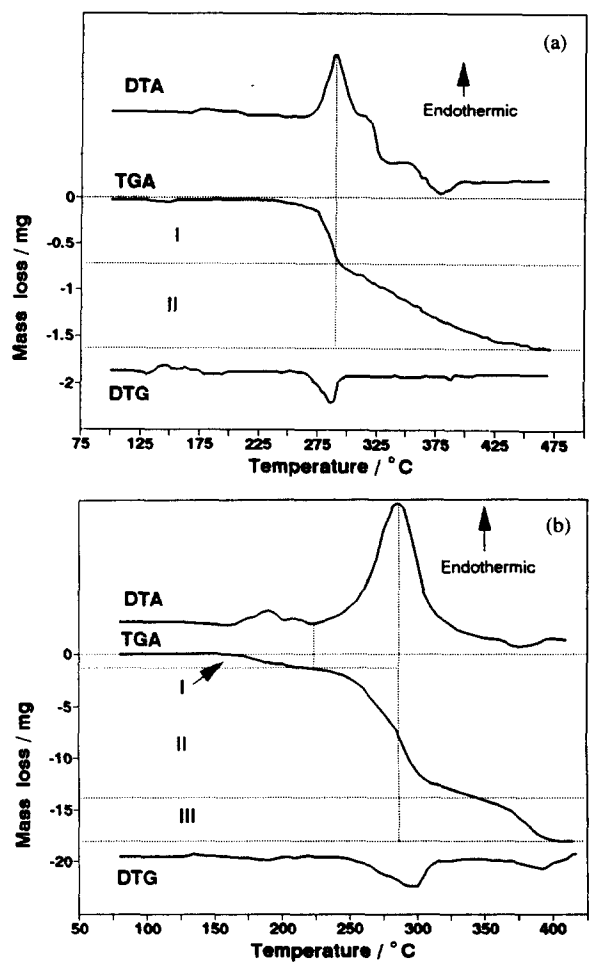

Fig. 2. (a) TGA, DTA and DTG of cathodic deposit $(NH_4)_{0.9}K_{3.1}V_6O_{16}$, scan rate 10 K/min, sample mass 55.27 mg. (b) TGA, DTA and DTG of cathodic deposit $(NH_4)_4V_6O_{16}$, scan rate 10 K/min, sample mass 100.4 mg. Base line for DTA is approximate. (For explanation of regions I to III, see text.)

region II where an oxidation-bulk recrystallization process occurred [10].

The alkali metal, M, present in the bronze limited the final oxidation step and non-stoichiometric V_2O_{5-y}-related materials were formed by this incomplete oxidation of V(IV) to V(V). The thermal decomposition in air of these electrodeposits have the overall reaction:

$$(NH_4)_xM_{4-x}V_6O_{16}+y/2O_2 \longrightarrow$$
$$M_{4-x}V_6O_{16+y-x/2}+xNH_3+x/2H_2O \quad (2)$$

The simultaneous DTA, DTG and TGA trace of $(NH_4)_4V_6O_{16}$ decomposed under an argon atmosphere is shown in Fig. 2(b). The DTA trace has three endothermic peaks at 193, 215 and 268 °C and one exothermic peak at 382 °C. The overall mass loss corresponds to the reaction:

$$(NH_4)_4V_6O_{16.0}\cdot 0.5H_2O \longrightarrow$$
$$V_6O_{13.77}+4NH_3+2.5H_2O+0.115O_2 \quad (3)$$

for which the net loss is 18.23%; the observed value from TGA is 18.3 mg on 100.4 mg sample, or 18.20%. In Fig. 2(b), region I marks the loss of hydrated water: 1.41% or 1.40 mg on 100.4 mg sample. The large endothermic DTA peak corresponded to the loss of the bulk of the NH_3 and H_2O in region II. Under an argon atmosphere, bulk oxidation of V(IV) to V(V) did not occur and the first reaction step is expected to be:

$$(NH_4)_4V_6O_{16} \longrightarrow (NH_4)_2V_6O_{15}+2NH_3+H_2O \quad (4)$$

The loss of NH_3 and H_2O continued and may result in the formation of a vanadium oxide with a stoichiometry close to that of V_3O_7 (if no reduction process occurred) by the reaction:

$$(NH_4)_2V_6O_{15} \longrightarrow V_6O_{14}+2NH_3+H_2O \quad (5)$$

Region III corresponded to the partial reduction of V(V) to V(IV) by the reaction:

$$V_6O_{14} \longrightarrow V_6O_{14-\delta}+\delta/2O_2 \quad (6)$$

where the value of δ was dependent on the amount of heating and oxygen partial pressure. For this specific example, chemical analysis gave $\delta=0.385$. It was not possible to separate the decomposition/reduction processes, which overlap over a 30 K range. The NH_3 is presumed to behave as a reducing agent so that some N_2 is formed by the reaction [10]:

$$(NH_4)_2V_6O_{15} \longrightarrow$$
$$V_6O_{14-3\delta}+2(1-\delta)NH_3+(1+3\delta)H_2O+\delta N_2 \quad (7)$$

Bernard et al. [11] observed that the decomposition of $(NH_4)_4V_6O_{16}$ formed V_6O_{13} but non-stoichiometric V_6O_{13} was probably formed, as observed in this work. The XRD spectra confirmed that our material was structurally similar to V_6O_{13} but slightly oxygen rich.

The decomposition of $(NH_4)_4M_{4-x}V_6O_{16}$ bronzes under inert atmospheres followed the steps given in Eqs. (4) to (7) and resulted in non-stoichiometric bronzes by the overall reaction:

$$(NH_4)_xM_{4-x}V_6O_{16} \longrightarrow$$
$$M_{4-x}V_6O_{16-y-x/2}+xNH_3+x/2H_2O+y/2O_2 \quad (8)$$

The reduction of the V(V) to V(IV) also depended on the ratio of M/V in the bronze.

3.2. Co-deposition of alkali metals and carbon

The possibility of co-depositing different alkali metals or carbon in the hexavanadate structure during electrodeposition was investigated. During electrodeposition in aqueous ammonium and alkali metal vanadate solutions the addition of a second alkali metal vanadate resulted in two alkali metals being included in the hexavanadate structure with the stoichiometry of

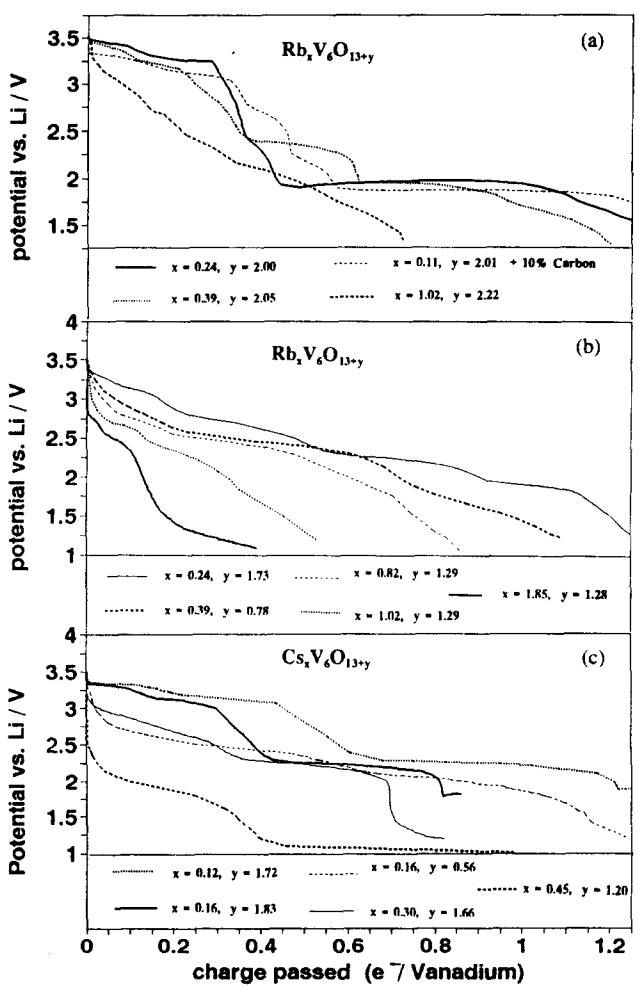

Fig. 3. Discharge potential vs. charge passed (e^-/V atom) for $M_xV_6O_{13+y}$ bronzes where (a) M = Rb and (b) Cs at 1 mA/cm^2 at various M/V ratios and vanadium oxidation states.

Table 1
Summary of analysis and reversible lithium insertion of the rubidium and cesium bronzes, $M_xV_6O_{13+\delta}$. Electrodes were discharged and charged by constant current with a current density from 0.5 to 2.0 cm^2 (to a 1.5 V cutoff voltage) in 0.5 M $LiClO_4$/propylene carbonate solutions

MVO_3 in solution (ml) [a]	M/V	Chemical analysis V(IV)/V(V)	$M_xV_6O_{13+y}$ [b]		Maximum Li inserted (e^-/V)	No. cycles and final capacity [c]
			x	y		
Rubidium						
2	0.018	0.015	0.11	2.01	1.18	5 (0.95)
3	0.040	0.041	0.24	2.00	1.10	20 (0.96)
3	0.040	0.130	0.24	1.73	1.15	10 (0.90)
5	0.065	0.050	0.39	2.05	0.95	15 (0.93)
5	0.065	0.472	0.39	0.78	0.98	25 (0.89)
10	0.137	0.374	0.82	1.29	0.79	30 (0.97)
20	0.170	0.098	1.02	2.22	0.70	20 (0.93)
20	0.170	0.407	1.02	1.29	0.45	35 (0.98)
30	0.308	0.548	1.85	1.28	0.32	45 (0.89)
Cesium						
5	0.020	0.113	0.12	1.72	1.19	10 (0.93)
10	0.027	0.085	0.16	1.83	0.79	15 (0.79)
10	0.027	0.507	0.16	0.56	1.06	20 (0.53)
20	0.050	0.163	0.30	1.66	0.69	27 (0.24)
35	0.075	0.342	0.45	1.20	0.33	10 (0.40)

[a] Value given are volume of standard 0.5 M MVO_3 added to saturated aqueous NH_4VO_3 to total volume of 0.25 l.
[b] Calculation of bronze stoichiometry assumes charge balance [10].
[c] Fraction of initial capacity on final discharge before analysis.

$(NH_4)_{4-(x+y)}M_xM'_yV_6O_{16}$ where M, M' = K, Rb or Cs and $x+y<4$. Upon thermal decomposition, a bronze with the stoichiometry $M_xM'_yV_6O_{13+\delta}$ was formed.

The inclusion of carbon during electrodeposition has been found to be possible by the addition of carbon powder at the appropriate time during the electrodeposition process. The cathodic deposition of hexavanadates is a complicated process in which a basic gradient of pH occurs at the cathode. When the required pH gradient is reached deposition occurs and the solution near the cathode changes from orange to a green colour [10]. About 0.2 g of carbon was stirred into the solution at this time and cyclic voltammetry was continued. The XRD patterns of the co-deposited carbon–vanadium oxide bronzes decomposed in air are not changed significantly except for a single major peak at 0.3367 nm ($2\theta = 26.449°$) which corresponded to carbon (graphite). Unlike K, Rb, Cs or NH_4, which are part of the hexavanadate structure [8], the co-deposited carbon was not part of the structure and was present more as an impurity.

3.3. Insertion of lithium

Phase changes that occurred during the discharge were dependent on the bronze stoichiometry. The rubidium and cesium bronzes could reversibly intercalate lithium similar to potassium bronzes [6,7]. Initial discharge curves of voltage plotted against charge passed (mol e^-/mol vanadium) for rubidium and cesium vanadium bronzes are shown in Fig. 3. Phase changes resembled those of V_2O_5 when $M/V \leqslant 0.05$. For $M/V \geqslant 0.1$, the initial flat voltage plateau at 3.3 V was shorter and the second plateau at about 2.4 V occurred at $e^-/V = 0.4$ to 0.45. The initial capacity for Li^+ to a 2.0 V cutoff voltage decreased proportionately with the amount of M^+ present in the bronze and the increased ionic size of M^+, due to the steric interference of the M^+ between the vanadium oxide layers. The reversible insertion of lithium was best when the depth-of-discharge was limited to 0.5 e^-/V. For $M/V \geqslant 0.15$, the phase changes were no longer distinct and the specific capacity dropped significantly (Table 1).

Initial discharge curves for the vacuum-decomposed bronzes (Fig. 3(b)) were similar to those of V_6O_{13} for $M/V < 0.05$ ($O/V < 2.3$) and the capacity for insertion decreased as the M/V ratio increased. The lower O/V ratio phases (higher V(IV)/V ratio) exhibited a greater reversible capacity. The number of cycles obtained until one half the initial capacity improved with increased M/V ratio for the lower O/V ratio bronzes (Table 1).

The potassium and rubidium bronzes both show a capacity increase over the first 10 cycles. Cyclic voltammograms of a rubidium bronze over the first 45 cycles are shown in Fig. 4(a). The capacity was still above the initial capacity after 45 cycles and the bronze electrode appeared to be stable in the PC electrolyte. Cycling resulted in a gradual shift of the oxidation and reduction peaks to higher voltages and a splitting of the single oxidation peak into two broader peaks was seen for both the potassium and rubidium bronzes.

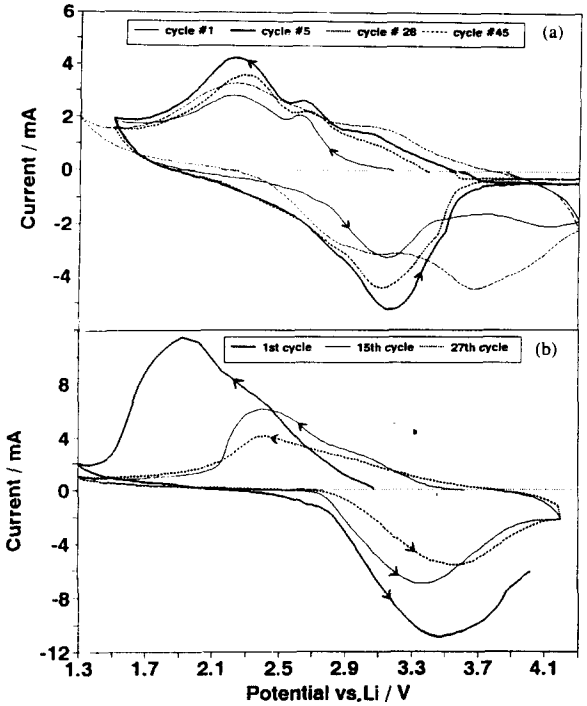

Fig. 4. Cyclic voltammetry of (a) a $Rb_xV_6O_{13+y}$ bronze, where $x=1.85$, $y=1.28$, and (b) a $Cs_xV_6O_{13+y}$ bronze, where $x=0.30$; $y=0.92$, at 1 mV/s for various cycle numbers.

The cesium bronzes had a significant capacity fade with cycling (Fig. 5(b)) and were thought to be impractical as cathode materials.

The cycling performance and discharge capacities of alkali metal bronzes containing co-deposited carbon were similar to those without carbon (Fig. 4(a)). No advantage was seen in co-depositing carbon with the bronzes possibly due to the nature of their formation on the substrate. The carbon behaved like an impurity which had an adverse effect on the adherence of the electrode material to the metal substrate which resulted in a decreased cycle life of the electrode. Formation of two co-deposited alkali metals to form $M_xM'_yV_6O_{13+\delta}$ bronzes also did not offer any advantages over the single alkali metal bronzes $M_yV_6O_{13+\delta}$. Specific capacities and phase changes were similar to single metal bronzes at comparable (M+M')/V ratios. However, by the electrodeposition method, a range of stoichiometries can be produced by changing the relative amounts of the meta-vanadates in the aqueous bath solution. A variety of bronzes can be created with increased deposit thickness to take advantage of their different properties.

The high solubility of vanadium oxides in the electrolyte is a problem. The addition of an alkali metal in the vanadium bronze appeared to improve the stability of the bronze in the PC electrolyte but the specific capacity was lowered in proportion to the M/V ratio.

4. Conclusions

The lithium insertion ability of the alkali metal vanadium oxides obtained by the thermal decomposition of $(NH_4)_xM_{4-x}V_6O_{16}$, was similar to V_2O_5 or V_6O_{13} for small M/V ratios and $M_4V_6O_{16}$ for large M/V ratios. Electrodes formed by heating in air with M/V=0.05 to 0.1 and O/V=2.4 to 2.5, gave the best cycle life. The electroformed bronzes show structures and properties unique to those prepared by high-temperature synthesis. The bronze structure and lithium insertion ability was influenced by the amount and ionic size of the alkali metal present.

References

[1] J. Desilvestro and O. Haas, *J. Electrochem. Soc., 137* (1990) 5C–22C.
[2] P. Hagenmuller, in J.C. Bailar, H.J. Emeleus, R. Nyholm and A.F. Trotman-Dickenson (eds.), *Comprehensive Inorganic Chemistry*, Vol. 4, Pergamon, London, 1973, pp. 569–601.
[3] I. Raistrick and R. Huggins, *Mater. Res. Bull., 18* (1983) 337.
[4] I. Raistrick, *Rev. Chim. Miner., 21* (1984) 456.
[5] J.P. Pereira-Ramos, R. Messina and J. Perichon, *J. Electrochem. Soc., 135* (1988) 3050–3057.
[6] E. Andrukaitis, *J. Power Sources, 43/44* (1993) 603.
[7] V. Manev, A. Momchilov, A. Nassalevska, G. Pistoia and M. Pasquali, *J. Power Sources, 43/44* (1993) 561.
[8] E. Andrukaitis, J.W. Lorimer and P.W.M. Jacobs, *Can. J. Chem., 68* (1990) 1283–1292.
[9] E. Andrukaitis, P.W.M. Jacobs and J.W. Lorimer, *Solid State Ionics, 27* (1988) 19.
[10] E. Andrukaitis, P.W.M. Jacobs and J.W. Lorimer, *Solid State Ionics, 37* (1990) 157.
[11] J. Bernard, F. Theobald and A. Vidonne, *Bull. Soc. Chim. Fr., 6* (1970) 2108.